ACS OMEGA

http://pubs.acs.org/journal/acsodf

Article

Sulfation of Diethylaminoethyl-Cellulose: QTAIM Topological Analysis and Experimental and DFT Studies of the Properties

Aleksandr Kazachenko,* Feride Akman, Mouna Medimagh, Noureddine Issaoui, Natalya Vasilieva, Yuriy N. Malyar, Irina G. Sudakova, Anton Karacharov, Angelina Miroshnikova, and Omar Marzook Al-Dossary

Cite This: *ACS Omega* 2021, 6, 22603−22615

Read Online

ACCESS | Metrics & More | Article Recommendations | Supporting Information

ABSTRACT: Sulfated cellulose derivatives are biologically active substances with anticoagulant properties. In this study, a new sulfated diethylaminoethyl (DEAE)-cellulose derivative has been obtained. The effect of a solvent on the sulfation process has been investigated. It is shown that 1,4-dioxane is the most effective solvent, which ensures the highest sulfur content in DEAE-cellulose sulfate under sulfamic acid sulfation. The processes of sulfamic acid sulfation in the presence of urea in 1,4-dioxane and in a deep eutectic solvent representing a mixture of sulfamic acid and urea have been compared. It is demonstrated that the use of 1,4-dioxane yields the sulfated product with a higher sulfur content. The obtained sulfated DEAE-cellulose derivatives have been analyzed by Fourier transform infrared spectroscopy, X-ray diffractometry, and scanning electron and atomic force microscopy, and the degree of their polymerization has been determined. The introduction of a sulfate group has been confirmed by the Fourier transform infrared spectroscopy data; the absorption bands corresponding to sulfate groups have been observed in the ranges of 1247−1256 and 809−816 cm^{-1}. It is shown that the use of a deep eutectic solvent leads to the side carbamation reactions. Amorphization of DEAE-cellulose during sulfation has been demonstrated using X-ray diffractometry. The geometric structure of a molecule in the ground state has been calculated using the density functional theory with the B3LYP/6-31G(d, p) basis set. The reactive areas of DEAE-cellulose and its sulfated derivatives have been analyzed using molecular electrostatic potential maps. The thermodynamic parameters (heat capacity, entropy, and enthalpy) of the target sulfation products have been determined. The HOMO−LUMO energy gap, Mulliken atomic charges, and electron density topology of the title compound have been calculated within the atoms in molecule theory.

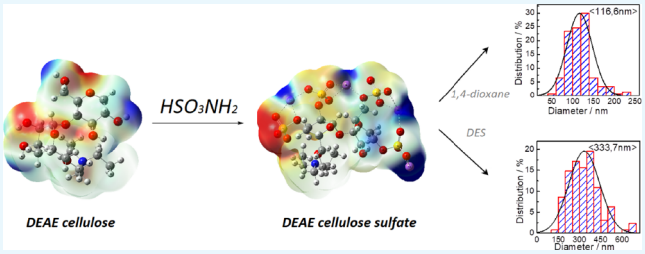

1. INTRODUCTION

Cellulose as the main structural component of lignocellulosic biomass is a valuable chemical raw material for production of highly demanded chemical compounds.[1]

Recently, an increasing number of cellulose-based functional materials have been developed. Lignocelluloses are used in bioethanol production;[1,2] sodium carboxymethyl cellulose serves as a new binder;[3] methyl, hydroxypropyl, and hydroxypropyl methyl celluloses are used as the basis of hydrogels;[4] cellulose fibers are in demand for alkaline batteries[5] and electrochemical capacitor separators.[6]

Cellulose-based materials, due to their unique properties, including excellent wettability, high porosity, light weight, biodegradability, and biocompatibility, find widespread application in food, pharmaceutical, and chemical industries as food additives,[7] thickeners,[8] pharmaceutical fillers,[9] emulsifiers,[10] etc.

Among numerous cellulose derivatives, the products containing sulfate groups attract special attention. Cellulose sulfates are used in industry as thickeners, sorbents, ion-exchange materials, etc.[11] The data on the physiological activity of such cellulose esters[12] expand the range of applications of sulfated cellulose (SC) in biochemical research and medicine.[13]

In the study by Torlopov and Frolova,[14] the sulfation of powdered celluloses with chlorosulfonic acid ($ClSO_3H$) in pyridine was carried out. The reaction proceeded at temperatures of 80−90 °C for 3 h. It was found that the increasing sulfation temperature is weakly related to a further increase in the degree of substitution (DS) but intensifies the polymer destruction. It was shown that the DS lies in the range of 0.06−0.47 in the sulfated powder celluloses obtained using an

Received: May 17, 2021
Accepted: August 12, 2021
Published: August 25, 2021

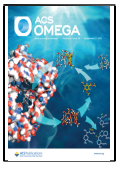

$AlCl_3$ acid catalyst and in the range of 1.21−1.76 in the sulfated powder celluloses obtained using the $TiCl_4$ catalyst.

In the study by Torlopov et al.,[15] the methods for obtaining the SC based on cotton microcrystalline cellulose (MCC) with the high DS were proposed and the properties of the products were investigated. The authors obtained the high DS by using a $ClSO_3H$−pyridine sulfating system with the formation of an intermediate SO_3−pyridine complex.[16] At reaction temperatures of 80−90 °C, the high-DS cellulose sulfates were synthesized. A further increase in the reaction temperature, along with an increase in the DS, enhanced the destruction of the polymer.

In the study by Wang et al.,[17] the synthesis methods, structure, and anticoagulant activity of the MCC sodium salt were discussed. The MCC sulfation carried out with the $ClSO_3H$−dimethylformamide complex under different conditions yielded the products with different DS values. The DS ranged between 0.6 and 1.7 and increased with the sulfating agent concentration. Studies of the anticoagulant activity opened prospects for the development of new drugs based on the MCC sulfate sodium salt.

The study by Wang et al.[18] was devoted to the use of ionic liquids, including 1-butyl-3-methylimidazolium chloride, 1-allyl-3-methylimidazolium chloride, and 1-ethyl-3-methylimidazolium acetate, as reaction media for homogeneous sulfation and as solvents for cellulose. Sulfation was performed with $ClSO_3H$ or the complexes of SO_3 with dimethylformamide (DMF) or pyridine in an ionic solution at 25 °C. In the solution of 1-ethyl-3-methylimidazolium acetate, acetylation occurred instead of the expected SC formation due to the participation of acetate ions in side reactions. The reaction proceeded for 30 min; a further increase in the reaction time did not increase the DS. The drawback of this method is a fairly long (up to 24 h) process of dissolving cellulose in the ionic solution at a high (80 °C) temperature.

Cellulose esterification can also be carried out via acetosulfation (the simultaneous acetylation and sulfation of cellulose) with the subsequent elimination of acetyl fragments.[19] In ref 19d, acetosulfation was performed for 5 h at 40−70 °C in a mixture of $ClSO_3H$ and acetic anhydride in anhydrous DMF. The subsequent deacetylation was carried out with the 1 M ethanol solution of NaOH for 15 h. The resulting cellulose sulfates were dissolved in water and had a DS value of 0.21−0.97. The drawbacks of this method are the two-stage process, the long-time (15 h) deacetylation stage, and the need for toxic reagents (DMF and acetic anhydride).

The H_2SO_4, SO_3, and $ClSO_3H$ compounds widely used in the sulfation reactions are highly aggressive reagents, which require special equipment and thereby complicate the process. In contrast to the above-listed reagents, sulfamic acid (NH_2SO_3H) is a stable nonhygroscopic crystalline substance. Its strength as an acid is comparable with that of H_2SO_4. Sulfamic acid is commercially manufactured by reacting urea with oleum. Wagenknecht's team[20] reported on the experiments on the NH_2SO_3H sulfation of partially substituted cellulose acetates dissolved in DMF. It was found that NH_2SO_3H does not react with free OH groups of cellulose at room temperature. Cellulose sulfation with the NH_2SO_3H−N_2O_4−DMF system was also reported in ref 21. However, it turned out that the production of high-DS SC is prevented by the formation of water, which decomposes the ester groups of cellulose nitrite, causing the regeneration of OH groups, which are not subjected to sulfation by NH_2SO_3H under these conditions. The DS of the cellulose sulfates obtained by this method was lower than 0.40.

Huang's team[22] reported on sulfation of cotton cellulose impregnated with the NH_2SO_3H and urea solution in DMF by sintering. However, high-temperature sintering of cellulose leads to polymer degradation. As is known,[23] cellulose degrades upon heating with NH_2SO_3H, but, in the presence of urea, which plays the role of an activator, sulfation occurs satisfactorily.

Sirviö et al.[24] proposed a new method of sulfation of cellulose with the sulfamic acid/urea (SAA/U) mixture deep eutectic solvent. This synthesis method does not require toxic organic solvents to be used. However, during the synthesis, the side carbamation reactions were observed, the effect of which on the biological activity remains understudied.

Recently, several methods for synthesizing the sulfated derivatives of polysaccharides on the basis of a new approach have been proposed. In particular, Chen et al.[25] described a new method for sulfation of xylan in a flow-through unit and investigated its anticoagulant activity. In ref 26, xylan was treated with the $NaBH_4$ reducing agent, which enhanced the purity of the product.

It should be noted that the variety of available methods for obtaining SC esters is reduced to three or four fundamentally different basic techniques. The rest of the methods are simply an improvement of these few techniques and differ from each other only in details. However, this diversity reflects the search for an "ideal" method, which is still lacking. The choice of the esterification method that would be the best for the production of cellulose sulfate esters is dictated by a combination of factors, including, first of all, the product yield, DS, completeness of the reagent use, and simplicity of a hardware design.

The aim of this study was to synthesize a new cellulose derivative, diethylaminoethyl sulfate (DEAE) cellulose, and compare the preparation methods and reaction products using physicochemical techniques. To obtain more information about the molecular geometry, noncovalent interactions, and electronic properties of the DEAE-cellulose complex, the B3LYP/6-31 G(d, p) density functional theory (DFT) calculation was performed. The effect of solvation on the properties of the DEAE-cellulose compound was studied.

2. RESULTS AND DISCUSSION

2.1. Synthesis of Diethylaminoethyl-Cellulose Sulfates. The mechanism of sulfation of polysaccharides with sulfamic acid remains understudied. However, it was assumed[27] that, upon sulfation of alcohols, the reaction is first-order for sulfamic acid and zero-order for alcohol. The rate of the direct interaction of alcohols with sulfamic acid is lower than the rate of catalyzed sulfation because the S−N bond in sulfamic acid is stronger than that in the donor−acceptor complex.[27a]

The reactivity of sulfamic acid increases in the presence of basic organic catalysts, including pyridine, urea, thiourea, acetamide, and picoline.[27] Urea is the most effective agent. An increase in the reactivity of sulfamic acid in the presence of urea is explained by the formation of a donor−acceptor complex.[28]

https://doi.org/10.1021/acsomega.1c02570
ACS Omega 2021, 6, 22603−22615

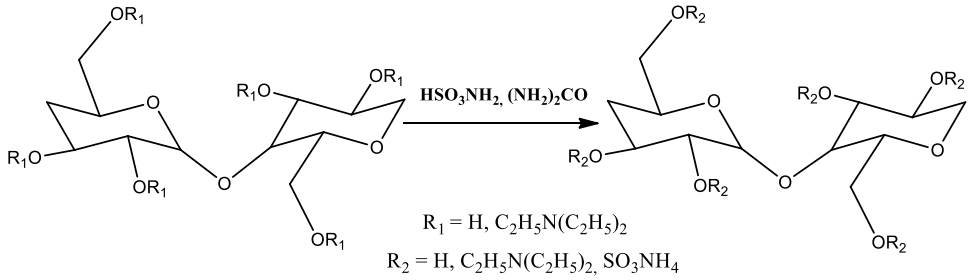

Figure 1. Scheme of the DEAE-cellulose sulfation reaction.

The reaction of DEAE-cellulose sulfation with the SAA/U complex occurred according to the scheme shown in Figure 1.

According to the data given in Table 1, the minimum sulfur content (7.2 wt %) in the reaction product during the sulfation of DEAE-cellulose with sulfamic acid in the presence of urea at 90 °C for 3.0 h is observed when morpholine is used as a solvent. The maximum sulfur content in the DEAE-cellulose sulfates is obtained using 1,4-dioxane.

Table 1. Effect of a Solvent on the Sulfur Content in DEAE-Cellulose Sulfates during Sulfation with Sulfamic Acid in the Presence of Urea at 90 °C for 3.0 h

no.	solvent	permittivity	K_b	sulfur content (wt %)
1	1,4-dioxane	2.3	1.2×10^{-17}	10.1
2	pyridine	12.5	1.5×10^{-9}	8.9
3	morpholine	7.3	2.1×10^{-6}	7.2
4	piperidine	5.9	1.3×10^{-3}	7.9
5	diglyme	7.4	2.0×10^{-18}	9.4

The sulfation reaction is conventionally described as a bimolecular nucleophilic substitution. It is well-known that the reactions proceeding by this mechanism are facilitated by aprotic solvents. When studying the effect of the nature of an aprotic solvent on the sulfation reaction rate, it is necessary to take into account the effect of the solvent on the entire process. First, the ability of these solvents to induce the ion-pair dissociation should increase with the permittivity, which, in turn, can lead to an increase in the rate of decomposition of sulfamic acid into ammonia and sulfur trioxide required in the sulfation reaction. Second, the basicity of a solvent noticeably affects the DS, which is related to the reactivity of the forming complex of sulfur trioxide and the corresponding solvent. The results given in Table 1 show that the sulfated product with the maximum sulfur content was obtained in the 1,4-dioxane medium. The process of sulfation of DEAE-cellulose in 1,4-dioxane medium using a solvent with the permittivity lower than that of the other solvents is characterized by a high sulfamic acid decomposition rate. Using sulfation of DEAE-cellulose in the solvents with a higher basicity as compared with dioxane (pyridine, morpholine, and piperidine), the less-sulfated DEAE-cellulose was obtained with the increasing solvent basicity. The sulfur content in the products of sulfation of DEAE-cellulose in ethers (dioxane and diglyme) with similar basic properties was almost the same (with a difference of less than 1 wt % for sulfur).

Thus, the data obtained showed the expedience of sulfation of DEAE-cellulose with sulfamic acid in 1,4-dioxane in the presence of urea.

According to the data given in Table 2, as the sulfation time increases, an increase in the sulfur content in the reaction products is observed. The comparison of the processes of DEAE-cellulose sulfation in 1,4-dioxane showed that the highest sulfur content in the reaction product is obtained with 1,4-dioxane. During sulfation of polysaccharides in the SAA/U deep eutectic solvent, the side reactions of carbamation of OH groups were observed,[24,29] which can also reduce the sulfur content in the DEAE-cellulose sulfate.

Table 2. Effect of the Process Conditions on the Sulfur Content in the DEAE-Cellulose Sulfate during Sulfation with Sulfamic Acid in the Presence of Urea at 90 °C

	sulfur content (wt %)	
time (h)	1,4-dioxane	deep eutectic solvent (SAA/U)
0.5	2.3	2.0
1	3.8	3.1
1.5	6.9	4.9
2	8.5	6.4
3	10.1	8.9
4	10.2	9.2

2.2. Fourier Transform Infrared Spectroscopy. The introduction of a sulfate group into the DEAE-cellulose molecule was confirmed by Fourier transform infrared (FTIR) spectroscopy (Figure 2). In the FTIR spectra of the sulfated DEAE-cellulose, absorption bands appear in the ranges of 1247−1256 and 809−816 cm^{-1}, which correspond to the sulfate group vibrations. It should be noted that, in sample SDEAE2, side carbamation reactions are observed, as evidenced by the appearance of absorption bands in the range of 1040−1065 cm^{-1} (−C−O−C− and CN) as well as at 1640 cm^{-1} (C═O).

2.3. X-ray Diffractometry. The comparison of X-ray diffraction patterns of the initial (SDEAE1) and sulfated (SDEAE2) DEAE-cellulose samples (Figure 3) shows that amorphization of the material is caused by disordering of the cellulose crystalline structure during sulfation.[19d30]

The X-ray diffraction pattern of the initial DEAE-cellulose sample contains peaks at Bragg angles of 14°−16°, 22.6°, and 34°−35°, which correspond to the crystal lattice characteristic of the cellulose-I structural modification.[31] The X-ray diffraction patterns of sample SDEAE1 have a similar shape with broader peaks at 2Θ = 14.0°, 22.7°, and 31.9°, respectively. In the X-ray diffraction pattern of sample SDEAE2, these peaks have a lower intensity and its structure can be considered close to amorphous.[32]

This is also indicated by the change in the crystallinity index calculated from the Segal formula,[31b] which decreases in the series 0.73 (DEAE-cellulose) > 0.53 (SDEAE1) > 0.21 (SDEAE2). The observed phenomenon is consistent with the literature data, according to which the use of the SAA/U

https://doi.org/10.1021/acsomega.1c02570
ACS Omega 2021, 6, 22603−22615

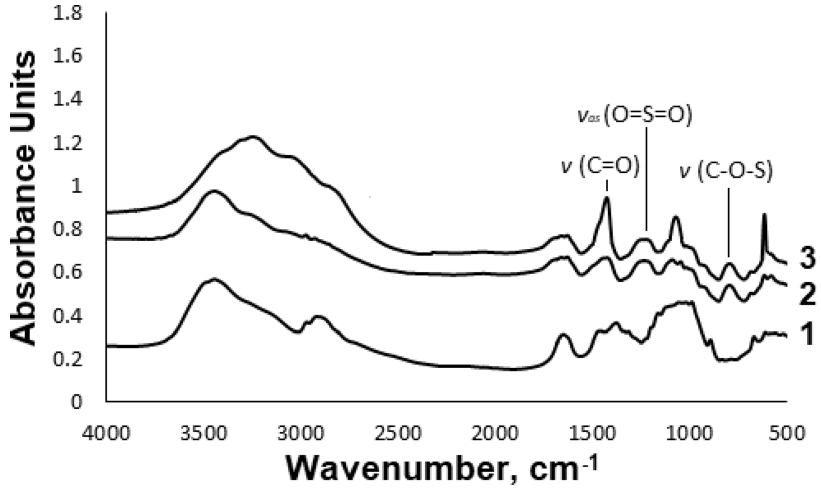

Figure 2. FTIR spectra of (1) initial DEAE-cellulose, (2) SDEAE1, and (3) SDEAE2.

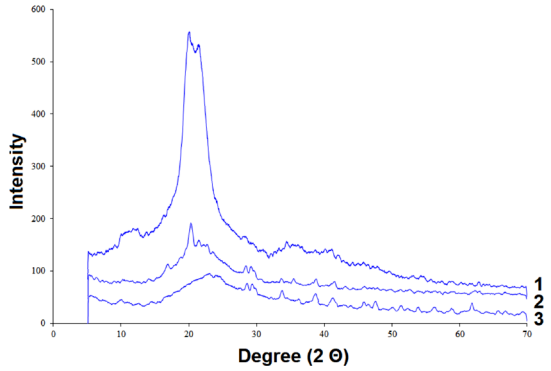

Figure 3. XRD data for (1) initial DEAE-cellulose, (2) SDEAE1, and (3) SDEAE2.

deep eutectic solvent leads to the stronger amorphization of polysaccharides[27a] than sulfation in organic solvents.[33]

Thus, according to the X-ray diffraction (XRD) data (Figure 3), in the process of sulfation of DEAE-cellulose, its further amorphization occurs. The data obtained agree with the results of the study.[34]

The obtained XRD data are consistent with the scanning electron microscopy (SEM) data (Figure 4). The SEM images show that the DEAE-cellulose fibrous structure is disordered during sulfation. The structural disordering is most pronounced in sample SDEAE2.

2.4. Scanning Electron Microscopy. According to the SEM data (Figure 4), DEAE-cellulose consists of filament-like tubular structures of different sizes. During sulfation, the DEAE-cellulose structure changes. The DEAE-cellulose sulfated with sulfamic acid in 1,4-dioxane consists of particles of different shapes and sizes, which form aggregates. For the DEAE-cellulose sulfated in the SAA/U deep eutectic solvent, the particles are smaller and do not form aggregates.

2.5. Atomic Force Microscopy. According to the atomic force microscopy (AFM) data (Figure 5), the surface of the DEAE-cellulose sulfate films obtained with sulfamic acid in 1,4-dioxane and the SAA/U deep eutectic solvent is homogeneous and contains no impurities. The particle sizes in the DEAE-cellulose sulfate film obtained in 1,4-dioxane and in the SAA/U deep eutectic solvent are 116.6 and 333.7 nm, respectively. According to the AFM images, sample SDEAE1 consists of homogeneous particles located close to each other and having a slightly elongated (elliptical) shape with an average diameter of 116 nm. In sample SDEAE2, the film surface consists of coarser particles and aggregates with an average diameter of about 333 nm, which are close to each other and have flat faces. Judging from the distribution diagram, they are less uniform in size than in sample SDEAE1. The surfaces of both film samples, according to the phase contrast images, have a homogeneous composition and contain no foreign inclusions; in other words, there are no inclusions of foreign substances, synthesis products, or other dissolved compounds on the film surface, which could crystallize on it upon drying the sample.

Thus, the AFM and XRD data unambiguously demonstrated that the synthesis conditions affect not only the size and monodispersity of the obtained sulfated DEAE-cellulose particles but also the degree of their crystallinity.

2.6. Gel Permeation Chromatography. Figure 6 shows the molecular weight distribution (MWD) curves for the DEAE-cellulose samples sulfated with sulfamic acid in 1,4-dioxane (curve 1) and the SAA/U deep eutectic solvent (curve 2). The curves are significantly different, which suggests different mechanisms of the processes occurring during sulfation of DEAE-cellulose. The DEAE-cellulose sulfated with sulfamic acid in 1,4-dioxane is characterized by a narrow MWD peak, which evidences for a fairly high homogeneity of the sample. This is also confirmed by the low (−1.18) polydispersity (Table 3). The DEAE-cellulose sulfated in the SAA/U deep eutectic solvent is characterized by a broad MWD peak, which shifts to the low-molecular weight region and is indicative of a higher (1.40) polydispersity and a low molecular weight (M_w = 19 861 g/mol). Such a change in the MWD curve can point out partial depolymerization of DEAE-cellulose during sulfation in the deep eutectic solvent. Since both the initial DEAE-cellulose and the synthesized product are soluble in the deep eutectic solvent, we can speak about the homogeneous process, when the reaction product is exposed to an aggressive environment throughout the process time, which leads to the rupture of glycosidic bonds. This is indirectly evidenced by the lower (9.2 wt %.) sulfur content. Probably, the low-molecular weight product with the high content of sulfate groups is removed during dialysis (Table 3).

2.7. Degree of Polymerization. In ref 35, the DS at the amino group in DEAE-cellulose molecules was found to be up to 0.95; therefore, the molecular weight of a polymer unit is about 251 g/mol. Taking into account the addition of sulfate

https://doi.org/10.1021/acsomega.1c02570
ACS Omega 2021, 6, 22603−22615

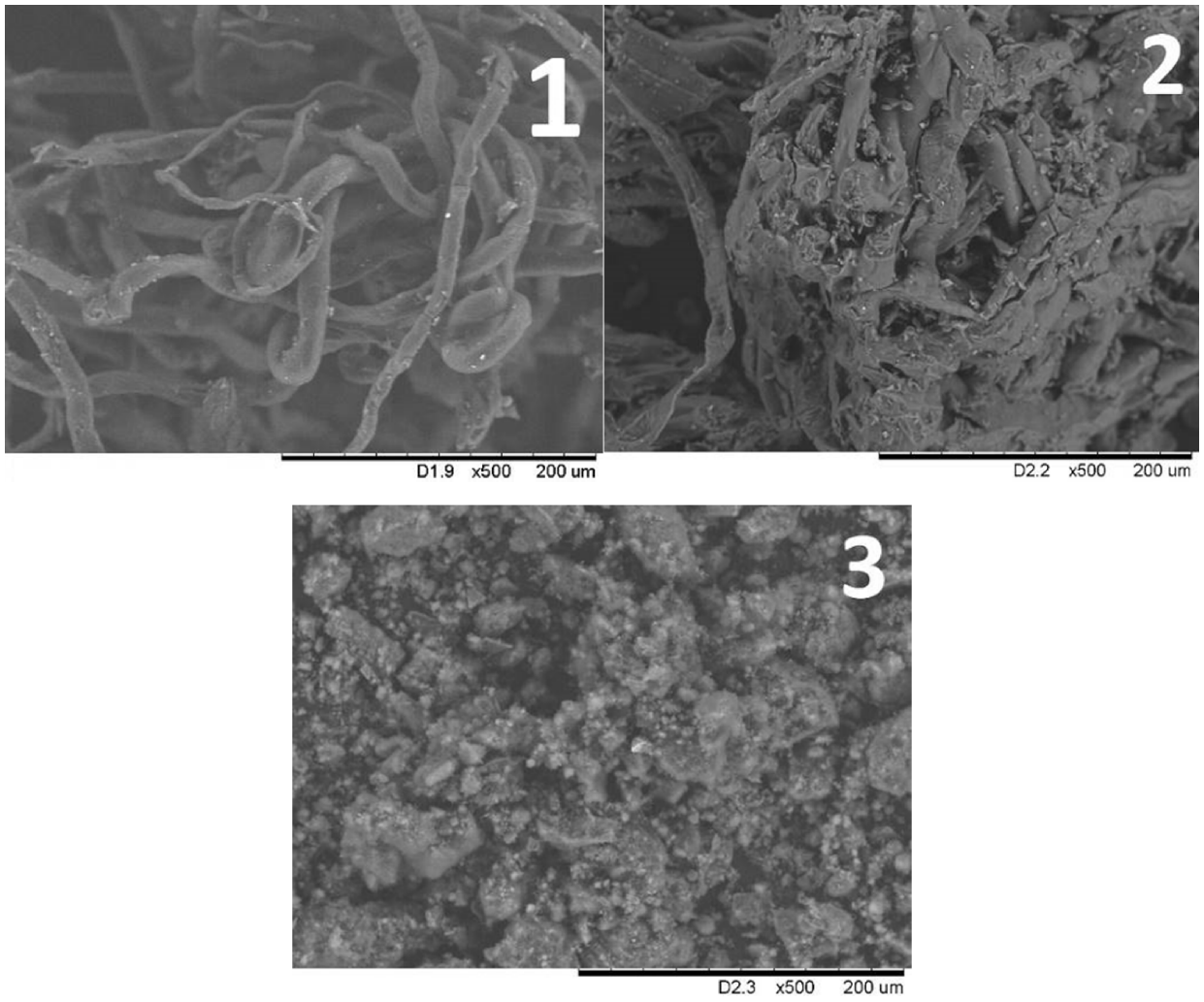

Figure 4. SEM images of (1) initial DEAE-cellulose, (2) SDEAE1, and (3) SDEAE2.

groups to free hydroxyls and a sulfur content of about 10 wt %, the molecular weight of the sulfated DEAE-cellulose unit is 342 g/mol, which was shown by elemental analysis. The obtained degree of polymerization (DP) data are given in Table 4.

According to the data given in Table 4, the highest DP value (84) corresponds to sample SDEAE1 synthesized in 1,4-dioxane. The DP value of sample SDEAE2 is 58, i.e., lower by a factor of 1.4. The lower DP of sample SDEAE2 can be related to depolymerization and partial hydrolysis of DEAE-cellulose during sulfation in the SAA/U deep eutectic solvent.

Thus, the obtained data are in good agreement with the data of gel permeation chromatography, which show that the M_w value for sample SDEAE1 is higher than that for sample SDEAE2 by a factor of 1.4, as well as with the XRD and SEM data.

2.8. Calculated Characteristics of DEAE-Cellulose and Its Sulfated Derivatives. *2.8.1. Molecular Electrostatic Potential Analysis of DEAE-Cellulose and Its Sulfated Derivatives.* The molecular electrostatic potential (MEP) maps were built to evaluate the modes of nucleophilic and electrophilic attacks and interactions of hydrogen compounds in DEAE-cellulose and its sulfated derivatives (Figure 7).[36] Different colors in the MEP map surface correspond to different values of the electrostatic potential. The decreasing potential is shown as blue > green > yellow > orange > red. The negative MEP values shown in red correspond to the electrophilic attack region and mostly on oxygen atoms in the sulfate groups. The nucleophilic attack region (positive) is shown in blue and mostly on sodium atoms and hydrogen atoms attached to oxygen atoms.[36] The high electronegativity of the sulfate groups leads to the highest reactivity in the sulfated-DEAE-cellulose derivatives.

It can be seen in Figure 7 that the electron density of oxygen atoms is higher (shown in reddish yellow in the map) than the electron density of hydrogen atoms attached to oxygen atoms (shown in blue in the map). When more sulfate groups are added to the DEAE-cellulose molecule, the MEP maps change. When the hydrogen atoms attached to oxygen are replaced by the sulfate groups, the blue color in the map gradually brightens according to a decrease in the amount of acidic hydrogens in the DEAE-cellulose molecule; however, the blue color in the map gradually brightens, which is also according to an increase in the number of sodium atoms. In the sulfated DEAE-cellulose derivatives, the blue color covers sodium atoms.

2.8.2. Calculated Electronic and Thermodynamic Properties of DEAE-Cellulose and Its Sulfated Derivatives. According to the data given in Table 5, the introduction of a sulfate group into the DEAE-cellulose molecule decreases the

https://doi.org/10.1021/acsomega.1c02570
ACS Omega 2021, 6, 22603−22615

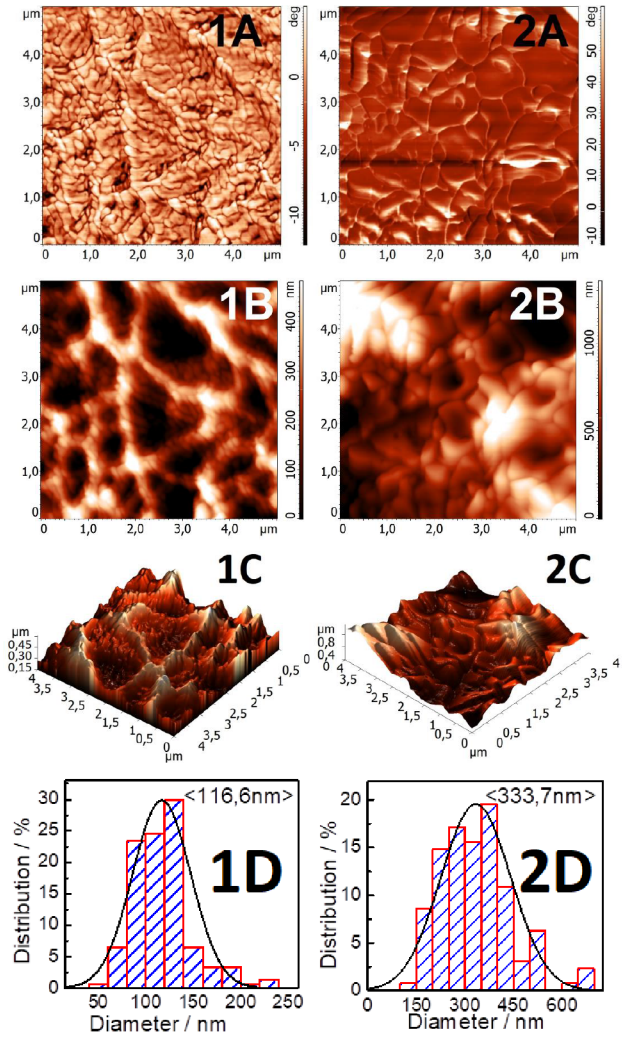

Figure 5. AFM data for (1) SDEAE1 and (2) SDEAE2 (A is the phase contrast, B is the relief, C is the 3D relief, and D is the particle size distribution).

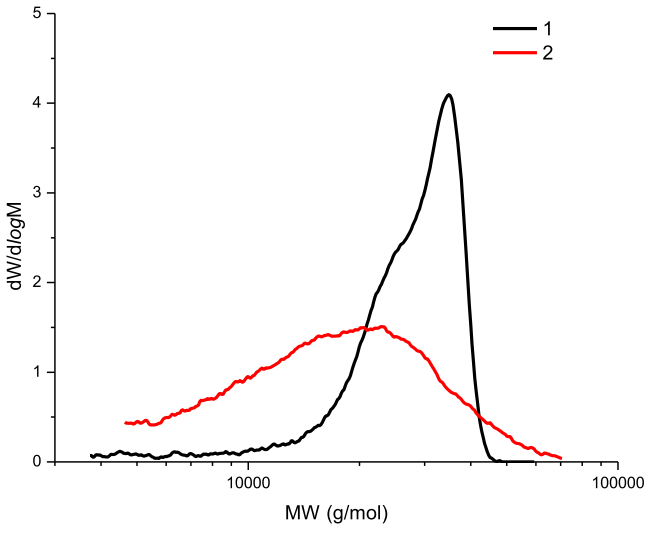

Figure 6. MWDs for (1) SDEAE1 and (2) SDEAE2.

E (RB3LYP) value by 786 (au); the introduction of more sulfate groups leads to a decrease in the *E* (RB3LYP) value by 786 (au) for each sulfate group on average, i.e., down to 4581.0740 (au).

Table 3. Molecular Weight Characteristics of the Sulfated DEAE-Cellulose Samples: Weight-Average Molecular Weight M_w, Number-Average Molecular Mass M_n, and Polydispersity PD (M_w/M_n)

sample	M_p (g/mol)	M_n (g/mol)	M_w (g/mol)	PD
SDEAE1	34 903	23 645	27 885	1.18
SDEAE2	22 917	14 196	19 861	1.40

Table 4. Effect of the DEAE-Cellulose Sulfation Conditions on the DP of the Obtained Products

sample	DP
SDEAE1	81
SDEAE2	58

The thermal energy increases almost linearly from 364.154 to 388.627 kcal/mol as the number of sulfate groups in DEAE-cellulose sulfate increases, and the introduction of one sulfate group leads to an increase in the thermal energy by 6 kcal/mol on average.

With an increase in the content of sulfate groups in the DEAE-cellulose sulfates, the enthalpy for each sulfate group increases by 6 kcal/mol on average. Thus, the initial DEAE-cellulose has an enthalpy of 364.746 kcal/mol and the sulfated DEAE-cellulose with four sulfate groups has an enthalpy of 389.2199 kcal/mol.

It can be seen in Table 5 that the entropy increases with the number of sulfate groups in the DEAE-cellulose molecule. The initial DEAE-cellulose has an entropy of 200.780 cal/mol K, and the DEAE-cellulose sulfate has an entropy of 301.696 cal/mol K.

The heat capacity also increases with the number of sulfate groups in the DEAE-cellulose molecule. In addition, Table 5 shows the most important dipole moment values observed for DEAE-cellulose-Sul4 (25.9006 D).

Thus, the introduction of a sulfate group into the DEAE-cellulose molecule leads to a regular increase in the *E* (thermal) value, dipole moment, enthalpy, entropy, and heat capacity and a decrease in the *E* (RB3LYP) value.

2.8.3. HOMO–LUMO Analysis of DEAE-Cellulose and Its Sulfated Derivatives. The frontier molecular orbital (FMO) theory helps understand the chemical stability and reactivity of a molecule.[37] It analyzes the electronic transition between the HOMO and LUMO frontier molecular orbitals.[38] Generally, the HOMO (as an electron donor) is the highest occupied molecular orbital and the LUMO (as an electron acceptor) is the lowest unoccupied molecular orbital.[36] The HOMO–LUMO energy difference is known as the energy band gap. The HOMO and LUMO 3D data on DEAE-cellulose and its sulfated derivatives are shown in Figure 8. Using the HOMO–LUMO energy gap, the electronegativity (χ), electron affinity (EA), chemical potential (μ), ionization potential (IP), hardness (η), softness (ς), electrophilicity index (ω), and maximum charge-transfer index (ΔN_{max}) were calculated (Table 6). These chemical parameters are defined by Koopmans' theorem,[39] which were calculated in the B3LYP/6-31G(d, p) basis set. The chemical softness (ς) is reciprocal to the chemical hardness (η) and determines the ability of an atom or a group of atoms to accept electrons; in addition, the chemical hardness (η) describes the resistance of an electron to

https://doi.org/10.1021/acsomega.1c02570
ACS Omega 2021, 6, 22603–22615

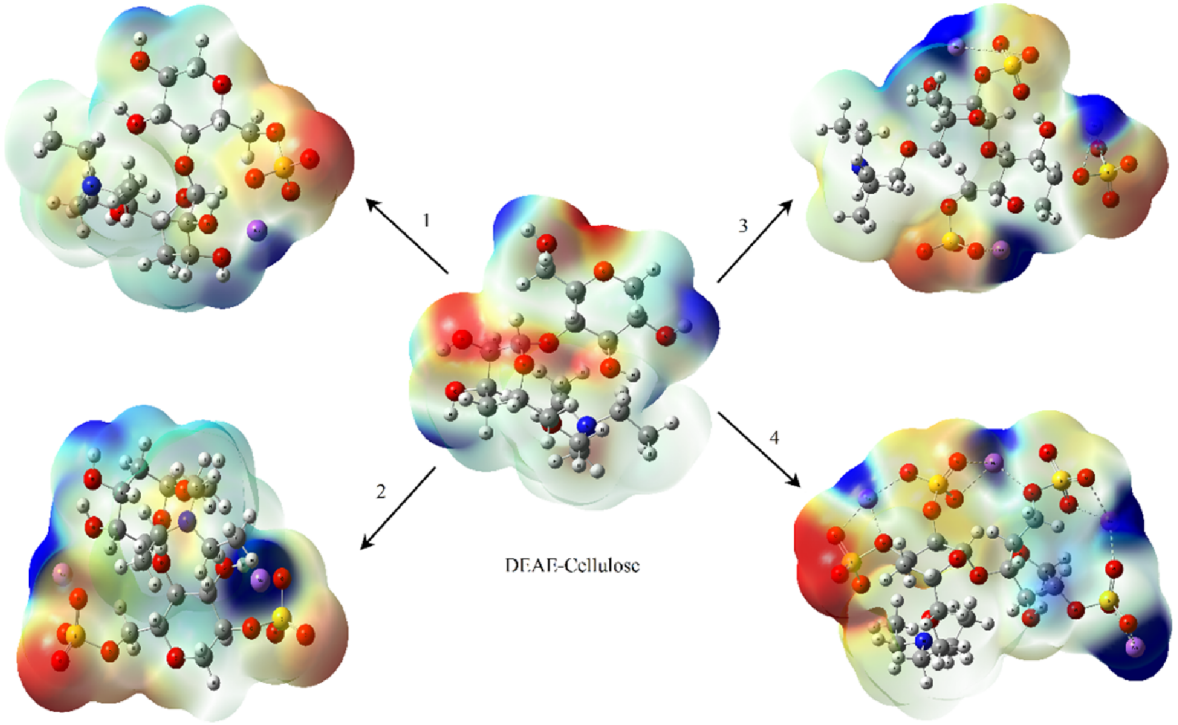

Figure 7. MEP maps of DEAE-cellulose and its sulfates with different contents of the sulfate groups (1−4).

Table 5. Calculated Electronic and Thermal Energies, Dipole Moment (μ), Entropy, Enthalpy, and Heat Capacity of DEAE-Cellulose and Its Sulfates (1−4) at 298.15 K and 1 atm

	DEAE-cellulose	DEAE-cellulose-Sul1	DEAE-cellulose-Sul2	DEAE-cellulose-Sul3	DEAE-cellulose-Sul4
E (RB3LYP) (au)	−1438.7118	−2224.3197	−3009.8979	−3795.4918	−4581.0740
μ (D)	2.6675	11.3010	16.6194	11.0917	25.9006
E (thermal) (kcal/mol)	364.154	370.362	376.74	382.618	388.627
enthalpy (kcal/mol)	364.746	370.955	377.3393	383.2115	389.2199
entropy (cal/mol K)	200.780	221.631	247.252	277.407	301.696
heat capacity (cal/mol K)	116.228	133.365	149.837	168.483	187.011

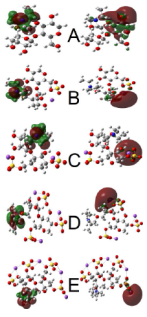

Figure 8. FMO for DEAE-cellulose and its sulfates with different contents of sulfate groups (1−4): (A) DEAE-cellulose, (B) DEAE-cellulose-Sul1, (C) DEAE-cellulose-Sul2, (D) DEAE-cellulose-Sul3, and (E) DEAE-cellulose-Sul4.

charge transfer.[40] The electronegativity (χ) is a measure of attraction of an atom or a group of atoms to electrons.[40]

The energy gap (ΔE), electronegativity (χ), electron affinity (EA), chemical potential (μ), ionization potential (IP), hardness (η), softness (ς), electrophilicity index (ω), and maximum charge-transfer index (ΔN_{max}) of DEAE-cellulose and its sulfated derivatives were determined using the HOMO and LUMO energies, and these descriptors can be calculated using the following equations:

$$\mathrm{IP} = -E_{\mathrm{HOMO}} \tag{1}$$

$$\mathrm{EA} = -E_{\mathrm{LUMO}} \tag{2}$$

$$\chi = -\frac{1}{2}(E_{\mathrm{LUMO}} + E_{\mathrm{HOMO}}) \tag{3}$$

$$\mu = \frac{1}{2}(E_{\mathrm{LUMO}} + E_{\mathrm{HOMO}}) \tag{4}$$

$$\eta = \frac{1}{2}(E_{\mathrm{LUMO}} - E_{\mathrm{HOMO}}) \tag{5}$$

$$\zeta = \frac{1}{\eta} \tag{6}$$

$$\omega = \frac{\mu^2}{2\eta} \tag{7}$$

$$\Delta N_{\mathrm{max}} = -\frac{\mu}{\eta} \tag{8}$$

At a small energy band gap between the HOMO and LUMO, the molecule can be associated with the high chemical reactivity and polarizability, as well as the low kinetic stability.[41] In addition, the calculated values of the energy gap (ΔE) and the total energy (E (RB3LYP)) with and

https://doi.org/10.1021/acsomega.1c02570
ACS Omega 2021, 6, 22603−22615

Table 6. Some Electronic Properties of DEAE-Cellulose and Its Sulfates (1−4)

parameters (eV)	DEAE-cellulose	DEAE-cellulose-Sul1	DEAE-cellulose-Sul2	DEAE-cellulose-Sul3	DEAE-cellulose-Sul4
E_{HOMO}	−5.2640	−5.4709	−5.5647	−5.5707	−4.9821
E_{LUMO}	1.2656	−0.6982	−1.6346	−1.8199	−2.6313
energy band gap (ΔE)	6.5296	4.7726	3.9301	3.7508	2.3508
chemical potential (μ)	−1.9992	−3.0845	−3.5997	−3.6953	−3.8067
softness (ς)	0.3063	0.4191	0.5089	0.5332	0.8508
ionization energy (I)	5.2640	5.4709	5.5647	5.5707	4.9821
electron affinity (A)	−1.2656	0.6982	1.6346	1.8199	2.6313
electronegativity (χ)	1.9992	3.0845	3.5997	3.6953	3.8067
chemical hardness (η)	3.2648	2.3863	1.9651	1.8754	1.1754
electrophilicity index (ω)	0.6121	1.9936	3.2970	3.6406	6.1644
maximum charge-transfer index (ΔN_{max})	0.6124	1.2926	1.8318	1.9704	3.2387

without dispersion of DEAE-cellulose and its sulfates (1−4) are listed in Table S1. The analysis of this table shows that the dispersion has a remarkable effect on the overall energy but has a very minor effect on the gap energy. We note that the dispersion improves the values of the total energy of the molecules studied. Dispersion effect increases the values of the energies E (RB3LYP) with a value between 0.01 and 0.3 au. For the calculated energy gap, the results reveal that dispersion has no effect, namely, on the DEAE-cellulose and its sulfates (1−4), the values are almost similar.

Thus, the narrowest energy band gap ΔE (2.3508 eV) is observed for the DEAE-cellulose sulfate with four sulfate groups (Table 6). The negative chemical potential values in all of the compounds indicate that all molecules are stable. With an increase in the number of sulfate groups in the DEAE-cellulose molecule, the electronegativity increases to 3.8067 eV. In addition, as the energy band gap between the HOMO and LUMO narrows, the chemical hardness of the molecule decreases, the chemical softness increases, and the activity of the molecule grows. In view of the aforesaid and according to the data given in Table 6, we can state that DEAE-cellulose-Sul4 is the most active molecule.

As the electrophilicity and maximum charge-transfer indices increase, the molecule acts more like an electrophile.

According to the data given in Table 6, we can state that, as the number of sulfate groups in the DEAE-cellulose molecule increases, the electrophilic ability of the molecule gradually increases. At the same time, as the number of sulfate groups in the DEAE-cellulose molecule increases, an increase in the softness (ς) to 0.8508 eV, electron affinity (A) to 2.6313 eV, electronegativity (χ) to 3.8067 eV, and electrophilicity index (ω) to 6.1644 eV is observed.

It should be noted that an increase in the number of sulfate groups in the DEAE-cellulose molecule leads to an uneven change in the calculated characteristics. In particular, the softness (ς) increases by 0.0898 eV with an increase in the number of sulfate groups from one to two, whereas with an increase in the number of sulfate groups from three to four, it increases by 0.3176 eV.

2.8.4. Mulliken Atomic Charges of DEAE-Cellulose and Its Sulfated Derivatives. Different atomic charges (Mulliken atomic charges, natural population (NPA) charges, and charges of electrostatic potentials using a method based on the grid (CHELPG)) were used to analyze the charges between ground and excited states of molecules. These tools are very important parameters to describe the electron distribution and the chemical reactivity and to explore the electrostatic potential (electrophilic/nucleophilic) of the compounds. In addition, these methods predict the same trends, but the difference between these methods is that the Mulliken charge method is a good way to account for the differences in electronegativity of the atoms within the molecule.[42] Here, we are interested in the analysis of the Mulliken population methods. The Mulliken atomic charges of DEAE-cellulose and its sulfated derivatives were calculated using B3LYP/6-31G (d, p). The atomic charges of DEAE-cellulose and its sulfated derivatives (according to the analysis of the Mulliken population) are listed in Table S2. The Mulliken atomic charges are related to the vibrational properties of a molecule and affect the atomic charge effect, molecular polarizability, different aspects of the electronic structure, and many properties of molecular systems.[43]

The introduction of an additional sulfate group into the DEAE-cellulose structure leads to a change in the Mulliken atomic charges for most atoms (Table S2). For example, when a sulfate group is introduced into the initial DEAE-cellulose molecule, the values of the C4 atom increase from 0.4077e to 0.4261e. With a further increase in the number of sulfate groups to three, the value of Mulliken atomic charges for a specified atom decreases to 0.3999e. For nitrogen, the value of Mulliken atomic charges naturally increases from −0.4105e to −0.3969e with an increase in the number of sulfate groups.

2.8.5. Theoretical FTIR Analysis of DEAE-Cellulose and Its Sulfated Derivatives. The FTIR technique has been intensively adapted to determine the vibrational properties of the studied compound. The FTIR spectra contain absorption bands with variable relative intensities. For DEAE-cellulose and its sulfated derivatives, the theoretical FTIR spectra were calculated using the DFT method with the 6-31G (d, p) basis set (Figure 10).

2.8.5.1. C−H Vibration. In the theoretical FTIR spectra of DEAE-cellulose and its sulfated derivatives, the C−H stretching vibrations are observed in the range of 3017−2868 cm^{-1} (Figures 9 and 10). The theoretically scaled wavenumbers in the range of 2995−2868 cm^{-1} refer to the C−H stretching vibrations in the DEAE-cellulose ring. The C−H stretching vibrations in the ring of the DEAE-cellulose sulfated derivatives theoretically scaled the wavenumbers in the range of 3017−2918 cm^{-1}.

2.8.5.2. O−H Vibration. The stretching vibrations of the OH groups are observed in samples DEAE-cellulose, DEAE-cellulose-Sul1, DEAE-cellulose-Sul2, DEAE-cellulose-Sul3, and DEAE-cellulose-Sul4 in the ranges of 3676−3616, 3689−3537, 3676−3345, 3657−3324, and 3643 cm^{-1}, respectively. It can be seen in Figure 4 that the stretching vibrations of OH groups in DEAE-cellulose-Sul1, DEAE-cellulose-Sul2, DEAE-cellu-

https://doi.org/10.1021/acsomega.1c02570
ACS Omega 2021, 6, 22603−22615

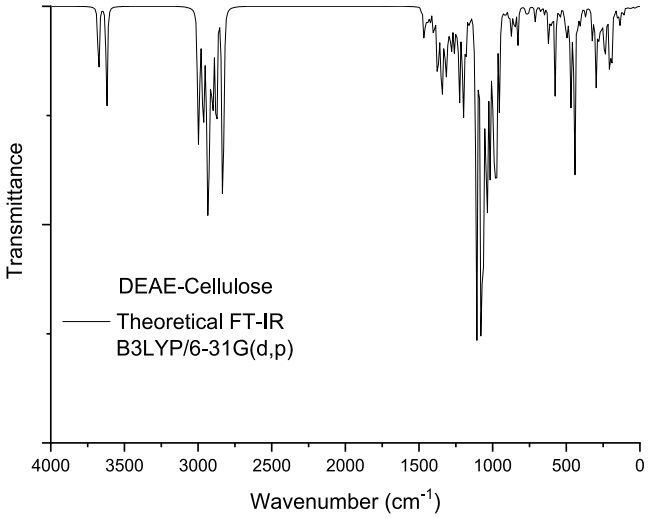

Figure 9. FTIR spectrum of DEAE-cellulose.

lose-Sul3, and DEAE-cellulose-Sul4 gradually shifted to the right with an increase in the number of sulfate groups and this region almost disappears according to the maximum displacement of the hydroxyl groups by the sulfate.

2.8.5.3. O−S Vibration. The theoretical calculation showed that the maximum intensity of the sulfate group vibrations is observed, in particular, in the range of 1280−1065 cm^{-1}.

It can be seen in Figure 10 that the O−S stretching vibrations in DEAE-cellulose-Sul1, DEAE-cellulose-Sul2, DEAE-cellulose-Sul3, and DEAE-cellulose-Sul4 are observed at 1252 and 1087 cm^{-1}; 1271, 1264, 1067, and 1065 cm^{-1}; 1257, 1253, 1242, 1150, 1145, and 1088 cm^{-1}; and 1234, 1216, 1175, 1167, 1163, 1133, 1123, and 1115 cm^{-1}, respectively.

For all the DEAE-cellulose sulfate samples with different numbers of sulfate groups, the FTIR spectra contain the absorption bands corresponding to the vibrations of sulfate groups in the ranges of 1142−1063, 1046−969, 740−714, and 571−485 cm^{-1}.[29,44]

2.8.5.4. C−C Vibration. The C−C vibrations in the aliphatic compounds are observed in the range of 1400−1650 cm^{-1}.[45] In the initial DEAE-cellulose, the C−C vibration occurs at wavenumbers of 1396−1352 cm^{-1}. In the DEAE-cellulose sulfate with different numbers of sulfate groups, the wavenumbers are 1402 cm^{-1} and 1341 cm^{-1}.

2.8.6. QTAIM Topological Analysis. To better understand the electronic structure of the systems, the quantum theory of atoms in molecule (QTAIM) method was used. This method,

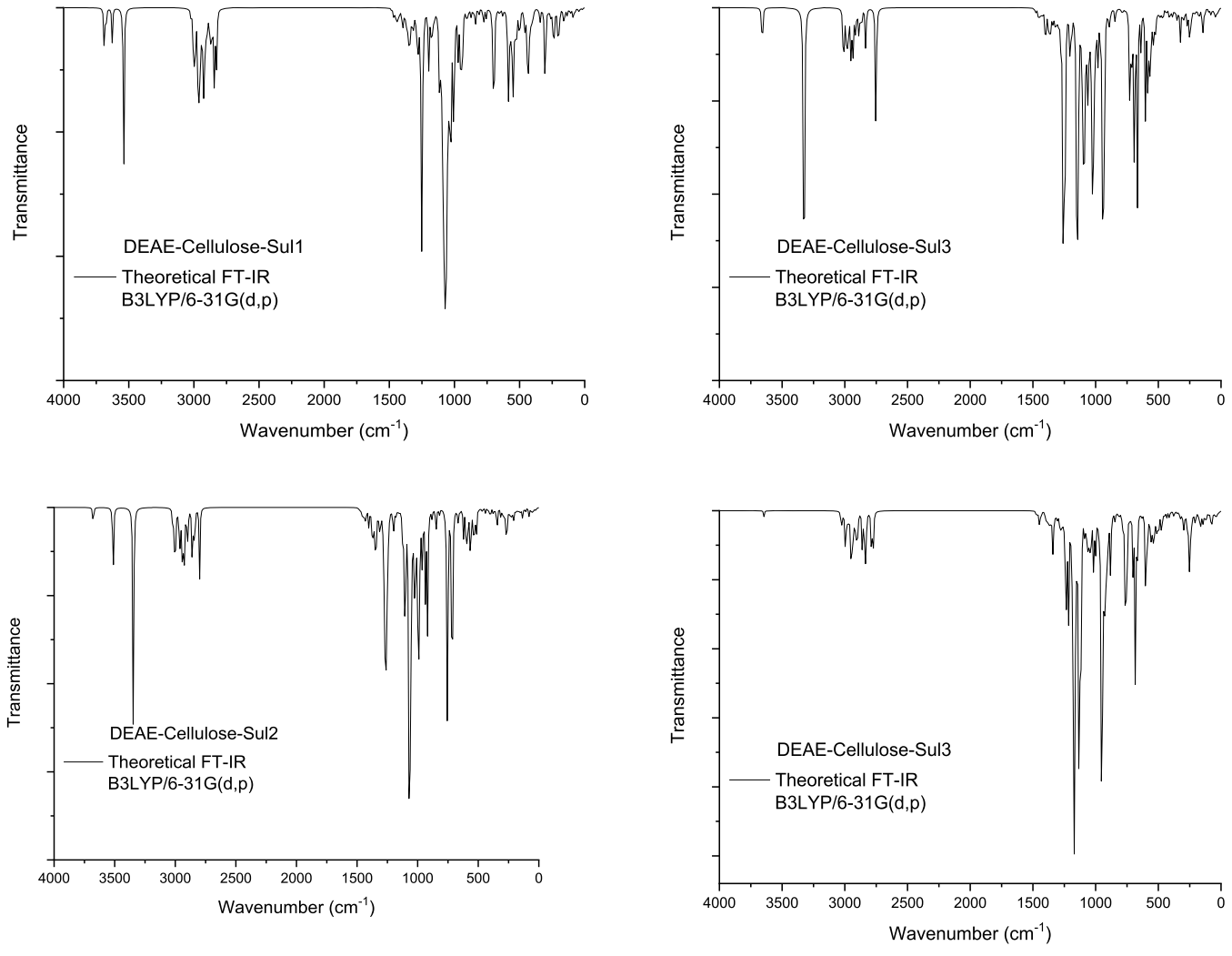

Figure 10. FTIR spectrum of the DEAE-cellulose sulfates with different numbers (1−4) of sulfate groups.

https://doi.org/10.1021/acsomega.1c02570
ACS Omega 2021, 6, 22603−22615

developed by Bader et al.,[46] allows one to make a topological description of a molecule. Later on, the AIM approach was applied to characterization of the bond interactions of a molecular complex and also allows the determination of critical points.[47] We can describe the liaison nature by the electron density $\rho(r)$, electron density Laplacian $\nabla^2\rho(r)$, kinetic energy density $G(r)$, potential energy density $V(r)$, interaction energy $E_{interactions}$, and the ratio $|V|/G$. In addition, the report $|V(r)|/G(r)$ makes it possible to characterize the nature of interactions: for covalent bonds, the ratio $|V(r)|/G(r)$ is greater than 2; for mixed character interactions, it is between 1 and 2; and for ionic bonds, the van der Waals interactions have a value of less than 1.[48] The topology analysis was carried out using the Multiwfn software;[48] the molecular surface maps for different DEAE-cellulose and its sulfate groups (1−4) are shown in Figure 11. In addition, we computed the topological

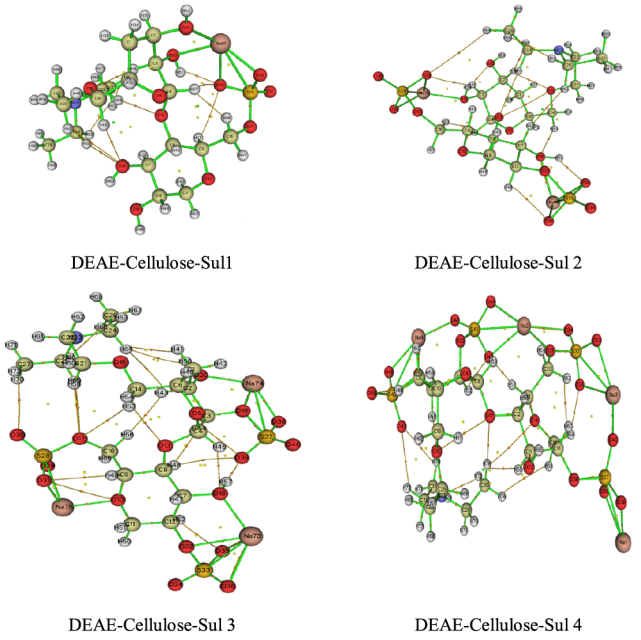

Figure 11. AIM molecular graph of DEAE-cellulose sulfate derivatives at B3LYP/6-31 G(d,p).

parameters at the BCP of the cation around the atoms; the results are gathered in Table S3. The ratio $|V(r)|/G < 1$, $H(r) > 0$ and $\nabla^2\rho(r) > 0$, is indicative of the closed-shell interactions typical of the ionic bonds and van der Waals interactions. Also, note that, according to the data reported in ref 49, all hydrogen bonds between DEAE-cellulose and its sulfated derivatives are considered to be weak since the Laplacian and the energy density values are positive.

3. CONCLUSIONS

The cellulose sulfated derivatives have different types of biological activities, including anticoagulant activity. Currently, cellulose acetate sulfate is the only known substance with the anticoagulant activity and electrolytic effects. In this study, we obtained a new mixed ether—diethylaminoethyl-cellulose sulfate—by two methods, specifically, sulfation of DEAE-cellulose with sulfamic acid in organic solvents and in the SAA/U deep eutectic solvent. It was shown that, in the first case, the target product with a higher sulfur content is obtained. In addition, we showed that 1,4-dioxane is the best solvent for sulfation of DEAE-cellulose with sulfamic acid. It was demonstrated that the method for synthesizing the DEAE-cellulose sulfates affects their structure, morphology, DP, and MWD. In addition, the quantum-chemical calculations were carried out; it was shown how the degree of sulfation affects the thermodynamic and topological characteristics of the target product. We believe that the new DEAE-cellulose sulfate compounds obtained by us can exhibit the biological activity and electrolytic effects due to the presence of both the sulfate and alkyl-amine groups.

4. EXPERIMENTAL SECTION

All chemicals were purchased from commercial suppliers. Reakhim DEAE-cellulose (Biokhimreaktiv, Russia) and sulfamic acid, urea, 1,4-dioxane, pyridine, diglyme, morpholine, and piperidine (Khimreaktivsnab, Russia) were used.

4.1. Sulfation of DEAE-Cellulose in Organic Solvents. DEAE-cellulose was sulfated with sulfamic acid in organic solvents (1,4-dioxane, pyridine, diglyme, morpholine, and piperidine) in the presence of urea. To do this, 50 mL of dioxane, 6.2 g of sulfamic acid, and 3.8 g of urea were placed in a three-necked flask equipped with a thermometer, a mechanical stirrer, and a thermostat, the resulting mixture was heated under vigorous stirring to 50 °C, and 1.5 g of air-dry DEAE-cellulose was added. Then, the temperature of the reaction mixture was raised to a constant value (see the sulfation conditions in Table 1) and stirred for 0.5−4 h. At the end of sulfation, the solvent was decanted, the resulting viscous residue was dissolved in 25 mL of water, and the excess sulfamic acid was neutralized with the 25% aqueous ammonia solution until it became neutral and poured into 100 mL of ethanol.

4.2. Sulfation of DEAE-Cellulose in a Deep Eutectic Solvent. DEAE-cellulose was sulfated using a modified procedure[24,29] in a three-necked flask in a deep eutectic solvent, which was the SAA/U mixture. For this purpose, sulfamic acid (12.4 g) was mixed with urea (7.6 g) and heated to 90 °C. DEAE-cellulose (1.5 g) was added to the obtained liquid deep eutectic solvent. The reaction occurred for 3 h. When the process was completed, the resulting mixture was dissolved in the 10% aqueous solution of ammonia (25 mL) and poured into 100 mL of ethanol.

4.3. Purification of the DEAE-Cellulose Sulfate. The viscous product obtained as described in sections 4.1 and 4.2 was separated and washed three times with 10 mL portions of ethanol until the formation of a solid precipitate. The precipitate representing the sulfated DEAE-cellulose derivative in the form of an ammonium salt was filtered off, washed on a filter with 10 mL of ethanol, and dried in air.

The sulfated DEAE-cellulose ammonium salt was purified by dialysis on cellophane against distilled water. The product was dialyzed for 10 h; water was changed in 1−2 h.

Hereinafter, we use the designations **SDEAE1** for the sulfated DEAE-cellulose obtained with sulfamic acid in 1,4-dioxane and **SDEAE2** for the sulfated DEAE-cellulose obtained in the SAA/U deep eutectic solvent.

4.4. Elemental Analysis. The elemental analysis of the sulfated DEAE-cellulose was performed on a FlashEA-1112 elemental analyzer (ThermoQuest, Italia).

4.5. Fourier Transform Infrared Spectroscopy. The FTIR spectra of the initial and sulfated DEAE-cellulose were recorded using a Shimadzu IR Tracer-100 spectrometer (Japan) within the wavelength range of 400−4000 cm^{-1}.

https://doi.org/10.1021/acsomega.1c02570
ACS Omega 2021, 6, 22603−22615

The spectral data were analyzed using the OPUS program (version 5.0). Solid samples for the analysis were prepared in the form of pills in a KBr matrix (2 mg sample/1000 mg KBr).

4.6. X-ray Diffraction. XRD analysis was carried out on a DRON-3 X-ray diffractometer (CuKα monochromatic radiation, λ = 0.154 nm) at a voltage of 30 kV and a current of 25 mA. The scanning step was 0.02°, and the intervals were 1 s per data point. The measurements were performed in the Bragg angle (2Θ) range from 5.00 to 70.00 Θ.

4.7. Scanning Electron Microscopy. SEM images were obtained on a Hitachi TM-1000 scanning electron microscope (Japan) at an accelerating voltage of 15 kV and a magnification from 100 to 10 000× with a resolution of 30 nm. The SEM images were treated using the ImageJ software (version 1.8.0_112).

4.8. Atomic Force Microscopy. AFM specimens of the sulfated DEAE-cellulose films were prepared as follows: the sulfated DEAE-cellulose (2 g) was dissolved in distilled water (30 mL) at room temperature. The resulting sulfated DEAE-cellulose solution was poured into a Petri dish and dried in an oven at a temperature of 45 °C to a constant weight. The obtained sulfated DEAE-cellulose films were separated from the Petri dish with tweezers and subjected to AFM analysis. The AFM study of the sulfated DEAE-cellulose films was carried out in a semicontact mode using a Solver P47 multimode scanning probe microscope (NT-MDT, Moscow) equipped with a 14 μm scanner and an adjustment stage (model SKM). In the semicontact AFM experiments, rectangular silicon cantilevers (NSG30, NT-MDT, Moscow) with an average resonance frequency of 320 kHz and a force constant of 40 N/m were used. The tip curvature radius was 10 nm.

4.9. Degree of Polymerization. The DP of the cellulose products was determined by measuring the specific viscosity of their solutions in a copper−ammonia complex using a capillary viscometer (VPZh-3, capillary diameter 0.56).[28,28,50]

4.10. Gel Permeation Chromatography (GPC). The weight-average molecular weight (M_w), number-average molecular weight (M_n), and polydispersity of the liquid product samples were determined by gel permeation chromatography using an Agilent 1260 Infinity II Multi-Detector GPC/SEC System with triple detection: refractometer, viscometer, and light scattering. The separation was performed on 2× Aquagel-OH mixed M and Aquagel OH-30 columns using a 0.1 M aqueous solution of $LiNO_3$ as a mobile phase. The column was calibrated using polydisperse PEG/PEO standards (Agilent, USA). The eluent flow rate was 1 mL/min, and the injected sample volume was 100 μL. Before the analysis, the samples were dissolved in the mobile phase (5 mg/mL) and filtered through a 0.45 μm PTFE membrane filter (Millipore). The data collection and processing were performed using the Agilent GPC/SEC MDS software.

4.11. Computational Details. Structural optimization is a necessary stage in obtaining the most stable structure of the compounds. In this study, all of the computations were performed in the Gaussian 09 program package[51] using the Gauss View 5.0.9 molecular imaging program[52] for the vapor phase. The B3LYP/6-31 G(d, p) DFT calculation was performed for DEAE-cellulose and a series of sulfates with one, two, three, and four sulfate groups, hereinafter referred to as DEAE-cellulose-Sul1, DEAE-cellulose-Sul2, DEAE-cellulose-Sul3, and DEAE-cellulose-Sul4, respectively.

To investigate the electrophilic and nucleophilic attacks and interactions of hydrogen bonds in the title molecule and its sulfate derivatives, MEP surface analysis was carried out. In addition, the electronic and thermodynamic properties were calculated. The FMO analysis was used to calculate the energy band gap and certain chemical parameters to predict the molecular reactivity of the investigated compounds. The theoretical FTIR spectra were calculated to determine the vibrational wavenumbers. The atoms in molecules (AIM) analysis was carried out using the Multiwfn software[53] to determine the topological properties at the bond critical points (BCPs).

■ ASSOCIATED CONTENT

Supporting Information

The Supporting Information is available free of charge at https://pubs.acs.org/doi/10.1021/acsomega.1c02570.

Dispersion effect on the energy band gap (ΔE) and the total energy, Mulliken atomic charges, and topological parameters of the bond critical points (PDF)

■ AUTHOR INFORMATION

Corresponding Author

Aleksandr Kazachenko − *Institute of Chemistry and Chemical Technology, Krasnoyarsk Science Center, Siberian Branch, Russian Academy of Sciences, Krasnoyarsk 660036, Russia; Siberian Federal University, Krasnoyarsk 660041, Russia;* orcid.org/0000-0002-3121-1666; Email: kazachenko.as@icct.krasn.ru

Authors

Feride Akman − *Vocational School of Food, Agriculture and Livestock, University of Bingöl, Bingöl 12000, Turkey*

Mouna Medimagh − *Laboratory of Quantum and Statistical Physics (LR18ES18), Faculty of Sciences, University of Monastir, Monastir 5079, Tunisia*

Noureddine Issaoui − *Laboratory of Quantum and Statistical Physics (LR18ES18), Faculty of Sciences, University of Monastir, Monastir 5079, Tunisia;* orcid.org/0000-0002-2350-7360

Natalya Vasilieva − *Institute of Chemistry and Chemical Technology, Krasnoyarsk Science Center, Siberian Branch, Russian Academy of Sciences, Krasnoyarsk 660036, Russia; Siberian Federal University, Krasnoyarsk 660041, Russia*

Yuriy N. Malyar − *Institute of Chemistry and Chemical Technology, Krasnoyarsk Science Center, Siberian Branch, Russian Academy of Sciences, Krasnoyarsk 660036, Russia; Siberian Federal University, Krasnoyarsk 660041, Russia*

Irina G. Sudakova − *Institute of Chemistry and Chemical Technology, Krasnoyarsk Science Center, Siberian Branch, Russian Academy of Sciences, Krasnoyarsk 660036, Russia*

Anton Karacharov − *Institute of Chemistry and Chemical Technology, Krasnoyarsk Science Center, Siberian Branch, Russian Academy of Sciences, Krasnoyarsk 660036, Russia*

Angelina Miroshnikova − *Institute of Chemistry and Chemical Technology, Krasnoyarsk Science Center, Siberian Branch, Russian Academy of Sciences, Krasnoyarsk 660036, Russia; Siberian Federal University, Krasnoyarsk 660041, Russia*

Omar Marzook Al-Dossary − *Department of Physics and Astronomy, College of Science, King Saud University, Riyadh 11451, Saudi Arabia*

Complete contact information is available at:
https://pubs.acs.org/10.1021/acsomega.1c02570

Author Contributions

A.K.: conceptualization, formal analysis, methodology, resources, supervision, writing original draft, review, and editing; F.A.: conceptualization, formal analysis, methodology, resources, writing original draft, review, and editing; M.M.: formal analysis, investigation, and writing original draft; N.I.: conceptualization, formal analysis, methodology, resources, supervision, writing original draft, review, and editing; N.V.: conceptualization, methodology, formal analysis, investigation, writing original draft, review, and editing; Y.N.M.: conceptualization, formal analysis, investigation, methodology, writing original draft, review, and editing; I.G.S.: methodology and writing original draft; A.K.: methodology, formal analysis, investigation, and writing original draft; A.M.: formal analysis and investigation; and O.M.A.-D.: conceptualization, formal analysis, review, and editing.

Notes

In the course of work in this article, the authors did not conduct research on animals and humans in any form.
The authors declare no competing financial interest.

■ ACKNOWLEDGMENTS

Experimental work was conducted within the framework of the budget plan no. 0287-2021-0017 for Institute of Chemistry and Chemical Technology SB RAS using the equipment of Krasnoyarsk Regional Research Equipment Center of SB RAS. Theoretical work was supported by Researchers Supporting Project number RSP-2021/61, King Saud University, Riyadh, Saudi Arabia. The authors are grateful to G.N. Bondarenko for the X-ray study and I.V. Korol'kova for recording the FTIR spectra.

■ REFERENCES

(1) Klemm, D.; Heublein, B.; Fink, H.; Bohn, A. Cellulose: Fascinating biopolymer and sustainable raw material. *Angew. Chem., Int. Ed. Engl.* **2005**, *44*, 3358−3393.
(2) Wu, Q.-X.; Guan, Y.-X.; Yao, S.-J. Sodium cellulose sulfate: A promising biomaterial used for microcarriers' designing. *Front. Chem. Sci. Eng.* **2019**, *13*, 46−58.
(3) Koo, B.; Kim, H.; Cho, Y.; Lee, K. T.; Choi, N.-S.; Cho, J. A Highly Cross-Linked Polymeric Binder for High-Performance Silicon Negative Electrodes in Lithium Ion Batteries. *Angew. Chem., Int. Ed.* **2012**, *51*, 8762−8767.
(4) Chang, C.; Zhang, L. Cellulose-based hydrogels: Present status and application prospects. *Carbohydr. Polym.* **2011**, *84*, 40−53.
(5) You, X.; Qiao, C.; Peng, D.; Liu, W.; Li, C.; Zhao, H.; Qi, H.; Cai, X.; Shao, Y.; Shi, X. Preparation of Alkaline Polyelectrolyte Membrane Based on Quaternary Ammonium Salt−Modified Cellulose and Its Application in Zn−Air Flexible Battery. *Polymers* **2021**, *13*, 9.
(6) Zhang, L.; Liu, Z.; Cui, G.; Chen, L. Biomass-derived materials for electrochemical energy storages. *Prog. Polym. Sci.* **2015**, *43*, 136−164.
(7) Andrade, D. R. M.; Mendonça, M. H.; Helm, C. V.; Magalhães, W. L. E.; De Muniz, G. I. B.; Kestur, S. G. Assessment of Nano Cellulose from Peach Palm Residue as Potential Food Additive: Part II: Preliminary Studies. *J. Food Sci. Technol.* **2015**, *52*, 5641−5650.
(8) García-Zapateiro, L. A.; Valencia, C.; Franco, J. M. Formulation of lubricating greases from renewable basestocks and thickener agents: A rheological approach. *Ind. Crops Prod.* **2014**, *54*, 115−121.
(9) Mousa, Z.; Anuar, M. S.; Taip, F.; Mohd Amin, M. C. I.; Tahir, S.; Mahdi, A. Deformation and Mechanical Characteristics of Compacted Binary Mixtures of Plastic (Microcrystalline Cellulose), Elastic (Sodium Starch Glycolate), and Brittle (Lactose Monohydrate) Pharmaceutical Excipients. *Part. Sci. Technol.* **2013**, *31*, 561−567.
(10) Ojala, J.; Sirviö, J. A.; Liimatainen, H. Nanoparticle emulsifiers based on bifunctionalized cellulose nanocrystals as marine diesel oil−water emulsion stabilizers. *Chem. Eng. J.* **2016**, *288*, 312−320.
(11) Lin, N.; Huang, J.; Dufresne, A. Preparation, properties and applications of polysaccharide nanocrystals in advanced functional nanomaterials: A review. *Nanoscale* **2012**, *4*, 3274−3294.
(12) Groth, T.; Wagenknecht, W. Anticoagulant potential of regioselective derivatized cellulose. *Biomaterials* **2001**, *22*, 2719−2729.
(13) Zhang, Q.; Lin, D.; Yao, S. Review on biomedical and bioengineering applications of cellulose sulfate. *Carbohydr. Polym.* **2015**, *132*, 311−322.
(14) (a) Torlopov, M. A.; Frolova, S. V. Preparation of powder materials by degradation of cellulose with Lewis's acids and their modification II. Sulfation of powder materials obtained by the destruction of cellulose with Lewis's acids. *Chem. Plant Raw Mater.* **2007**, *3*, 63−67. (b) Torlopov, M. A.; Frolova, S. V.; Demin, V. A. Sulphating of powder cellulose that was obtained by the catalytic destruction method by titanium tetrachloride. *Chem. Sustainable Dev.* **2007**, *15*, 483−488.
(15) Torlopov, M. A.; Demin, V. A. Sulfated and carboxymethylated derivatives of microcrystalline cellulose. *Chem. Plant Raw Mater.* **2007**, 55−61.
(16) Mähner, C.; Lechner, M.; Nordmeier, E. Synthesis and characterisation of dextran and pullulan sulphate. *Carbohydr. Res.* **2001**, *331*, 203−208.
(17) Wang, Z. M.; Li, L.; Zheng, B. S.; Normakhamatov, N.; Guo, S. Y. Preparation and anticoagulation activity of sodium cellulose sulfate. *Int. J. Biol. Macromol.* **2007**, *41*, 376−382.
(18) (a) Wang, Z.-M.; Li, L.; Xiao, K.-J.; Wu, J.-Y. Homogeneous sulfation of bagasse cellulose in an ionic liquid and anticoagulation activity. *Bioresour. Technol.* **2009**, *100*, 1687−1690. (b) Gericke, M.; Liebert, T.; Heinze, T. Interaction of Ionic Liquids with Polysaccharides, 8—Synthesis of Cellulose Sulfates Suitable for Polyelectrolyte Complex Formation. *Macromol. Biosci.* **2009**, *9*, 343−353.
(19) (a) Zhang, K.; Brendler, E.; Fischer, S. FT Raman investigation of sodium cellulose sulfate. *Cellulose* **2010**, *17*, 427−435. (b) Peschel, D.; Zhang, K.; Aggarwal, N.; Brendler, E.; Fischer, S.; Groth, T. Synthesis of novel celluloses derivatives and investigation of their mitogenic activity in the presence and absence of FGF2. *Acta Biomater* **2010**, *6*, 2116−2125. (c) Zhang, K.; Brendler, E.; Geissler, A.; Fischer, S. Synthesis and spectroscopic analysis of cellulose sulfates with regulable total degrees of substitution and sulfation patterns via 13C NMR and FT Raman spectroscopy. *Polymer* **2011**, *52*, 26−32. (d) Zhang, K.; Peschel, D.; Bäucker, E.; Groth, T.; Fischer, S. Synthesis and characterisation of cellulose sulfates regarding the degrees of substitution, degrees of polymerisation and morphology. *Carbohydr. Polym.* **2011**, *83*, 1659−1664.
(20) Wagenknecht, W.; Nehls, I.; Kotz, J.; Philipp, B.; Ludwig, J. Investigation of the sulfatation of partly substituted cellulose acetate under homogeneous conditions. *Cellul. Chem. Technol.* **1993**, *25*, 343−354.
(21) Wagenknecht, W.; Nehls, I.; Philipp, B. Studies on the regioselectivity of cellulose sulfation in an N_2O_4-*N*,*N*-dimethylformamide-cellulose system. *Carbohydr. Res.* **1993**, *240*, 245−252.
(22) Huang, X.; Zhang, W.-D. Preparation of Cellulose Sulphate and Evaluation of its Properties. *J. Fiber Bioeng. Inf.* **2010**, *3*, 32−39.
(23) Al-Horani, R. A.; Desai, U. R. Chemical Sulfation of Small Molecules—Advances and Challenges. *Tetrahedron* **2010**, *66*, 2907−2918.
(24) Sirviö, J. A.; Ukkola, J.; Liimatainen, H. Direct sulfation of cellulose fibers using a reactive deep eutectic solvent to produce highly charged cellulose nanofibers. *Cellulose* **2019**, *26*, 2303−2316.

(25) Chen, Y.; Sun, X.; Shan, J.; Tang, C.; Hu, R.; Shen, T.; Qiao, H.; Li, M.; Zhuang, W.; Zhu, C.; Ying, H. Flow synthesis, characterization, anticoagulant activity of xylan sulfate from sugarcane bagasse. *Int. J. Biol. Macromol.* **2020**, *155*, 1460−1467.
(26) Pfeifer, A.; Heinze, T. Synthesis of pyridine-free xylan sulfates. *Carbohydr. Polym.* **2019**, *206*, 65−69.
(27) (a) Kazachenko, A. S.; Malyar, Y. N.; Vasilyeva, N. Y.; Bondarenko, G. N.; Korolkova, I. V.; Antonov, A. V.; Karacharov, A. A.; Fetisova, O. Y.; Skvortsova, G. P. ≪Green≫ synthesis and characterization of galactomannan sulfates obtained using sulfamic acid. *Biomass Convers. Biorefin.* **2020**, DOI: 10.1007/s13399-020-00855-2. (b) Spillane, W.; Malaubier, J.-B. Sulfamic Acid and Its N- and O-Substituted Derivatives. *Chem. Rev.* **2014**, *114*, 2507−2586.
(28) Kuznetsov, B.; Levdansky, V.; Kuznetsova, S.; Garyntseva, N.; Sudakova, I.; Levdansky, A. Integration of peroxide delignification and sulfamic acid sulfation methods for obtaining cellulose sulfates from aspen wood. *Eur. J. Wood Wood Prod.* **2018**, *76*, 999−1007.
(29) Akman, F.; Kazachenko, A. S.; Vasilyeva, N. Y.; Malyar, Y. N. Synthesis and characterization of starch sulfates obtained by the sulfamic acid-urea complex. *J. Mol. Struct.* **2020**, *1208*, No. 127899.
(30) Yue, X.; Wu, Z.; Wang, G.; Liang, Y.; Sun, Y.; Song, M.; Zhan, H.; Bi, S.; Liu, W. High acidity cellulose sulfuric acid from sulfur trioxide: A highly efficient catalyst for the one step synthesis of xanthene and dihydroquinazolinone derivatives. *RSC Adv.* **2019**, *9*, 28718−28723.
(31) (a) Park, S.; Baker, J. O.; Himmel, M. E.; Parilla, P. A.; Johnson, D. K. Cellulose crystallinity index: Measurement techniques and their impact on interpreting cellulase performance. *Biotechnol. Biofuels* **2010**, *3*, No. 10. (b) Nam, S.; French, A. D.; Condon, B. D.; Concha, M. Segal crystallinity index revisited by the simulation of X-ray diffraction patterns of cotton cellulose Iβ and cellulose II. *Carbohydr. Polym.* **2016**, *135*, 1−9.
(32) Šimkovic, I.; Tracz, A.; Kelnar, I.; Uhliariková, I.; Mendichi, R. Quaternized and sulfated xylan derivative films. *Carbohydr. Polym.* **2014**, *99*, 356−364.
(33) Kazachenko, A. S.; Akman, F.; Sagaama, A.; Issaoui, N.; Malyar, Y. N.; Vasilieva, N. Y.; Borovkova, V. S. Theoretical and experimental study of guar gum sulfation. *J. Mol. Model.* **2021**, *27*, No. 5.
(34) (a) Levdansky, V. A.; Kondracenko, A. S.; Levdansky, A. V.; Kuznetsov, B. N.; Djakovitch, L.; Pinel, C. Sulfation of Microcrystalline Cellulose with Sulfamic Acid in N,N-Dimethylformamide and Diglyme. *J. Sib. Fed. Univ., Chem.* **2014**, *2*, 162−169. (b) Kazachenko, A. S.; Malyar, Y. N.; Vasilyeva, N. Y.; Fetisova, O. Y.; Chudina, A. I.; Sudakova, I. G.; Antonov, A. V.; Borovkova, V. S.; Kuznetsova, S. A. Isolation and sulfation of galactoglucomannan from larch wood (Larix sibirica). *Wood Sci. Technol.* **2021**, *55*, 1091−1107. (c) Romanchenko, A. S.; Levdansky, A. V.; Levdansky, V. A.; Kuznetsov, B. N. Study of cellulose sulfates by X-ray photoelectron spectroscopy. *Russ. J. Bioorg. Chem.* **2015**, *41*, 719−724.
(35) Liesiene, J.; Kazlauske, J. Functionalization of cellulose: Synthesis of water-soluble cationic cellulose derivatives. *Cellul. Chem. Technol.* **2013**, *47*, 515−525.
(36) (a) Akman, F. A density functional theory study based on monolignols: Molecular structure, HOMO-LUMO analysis, molecular electrostatic potential. *Cellul. Chem. Technol.* **2019**, *53*, 243−250. (b) Akman, F.; Kazachenko, A.; Malyar, Y. A density functional theory study of sulfated monolignols: p-coumaril and coniferyl alcohols. *Cellul. Chem. Technol.* **2021**, *55*, 41−54.
(37) Noureddine, O.; Gatfaoui, S.; Brandán, S. A.; Marouani, H.; Issaoui, N. Structural, docking and spectroscopic studies of a new piperazine derivative, 1-Phenylpiperazine-1,4-diium bis(hydrogen sulfate). *J. Mol. Struct.* **2020**, *1202*, No. 127351.
(38) Ben Issa, T.; Sagaama, A.; Issaoui, N. Computational study of 3-thiophene acetic acid: Molecular docking, electronic and intermolecular interactions investigations. *Comput. Biol. Chem.* **2020**, *86*, No. 107268.
(39) Gatfaoui, S.; Sagaama, A.; Issaoui, N.; Roisnel, T.; Marouani, H. Synthesis, experimental, theoretical study and molecular docking of 1-ethylpiperazine-1,4-diium bis(nitrate). *Solid State Sci.* **2020**, *106*, No. 106326.
(40) Ben M'leh, C.; Brandán, S. A.; Issaoui, N.; Roisnel, T.; Marouani, H. Synthesis, molecular structure, vibrational and theoretical studies of a new non-centrosymmetric organic sulphate with promising NLO properties. *J. Mol. Struct.* **2018**, *1171*, 771−785.
(41) Fleming, J. Frontier Orbitals andrganic Chemical Reactions. *J. Prakt. Chem.* **1978**, *320*, 879−880.
(42) Demircioğlu, Z.; Kaştaş, Ç. A.; Büyükgüngör, O. Theoretical analysis (NBO, NPA, Mulliken Population Method) and molecular orbital studies (hardness, chemical potential, electrophilicity and Fukui function analysis) of (E)-2-((4-hydroxy-2-methylphenylimino)-methyl)-3-methoxyphenol. *J. Mol. Struct.* **2015**, *1091*, 183−195.
(43) (a) Mulliken, R. S. Electronic Population Analysis on LCAO−MO Molecular Wave Functions. I. *J. Chem. Phys.* **1955**, *23*, 1833−1840. (b) Akman, F. A comparative study based on molecular structure, spectroscopic, electronic, thermodynamic and NBO analysis of some nitrogen-containing monomers. *Polym. Bull.* **2021**, *78*, 663−693.
(44) Rohowsky, J.; Heise, K.; Fischer, S.; Hettrich, K. Synthesis and characterization of novel cellulose ether sulfates. *Carbohydr. Polym.* **2016**, *142*, 56−62.
(45) Vasilyeva, N. Y.; Kazachenko, A. S.; Malyar, Y. N.; Kuznetsov, B. N. Sulfation of betulin with chlorosulfonic acid in pyridine. *J. Sib. Fed. Univ., Chem.* **2020**, *13*, 447−459.
(46) Bader, R. F. W. A Bond Path: A Universal Indicator of Bonded Interactions. *J. Phys. Chem. A* **1998**, *102*, 7314−7323.
(47) Bader, R. F. W. *Atoms in Molecules: A Quantum Theory*; Oxford University Press: Oxford, 1990.
(48) Tahenti, M.; Gatfaoui, S.; Issaoui, N.; Roisnel, T.; Marouani, H. A tetrachlorocobaltate(II) salt with 2-amino-5-picolinium: Synthesis, theoretical and experimental characterization. *J. Mol. Struct.* **2020**, *1207*, No. 127781.
(49) Jomaa, I.; Noureddine, O.; Gatfaoui, S.; Issaoui, N.; Roisnel, T.; Marouani, H. Experimental, computational, and in silico analysis of (C8H14N2)2[CdCl6] compound. *J. Mol. Struct.* **2020**, *1213*, No. 128186.
(50) Luo, C.; Wang, S.; Liu, H. Cellulose Conversion into Polyols Catalyzed by Reversibly Formed Acids and Supported Ruthenium Clusters in Hot Water. *Angew. Chem., Int. Ed.* **2007**, *46*, 7636−7639.
(51) Frisch, M. J.; Trucks, G. W.; Schlegel, H. B.; Scuseria, G. E.; Robb, M. A.; Cheeseman, J. R.; Scalmani, G.; Barone, V.; Mennucci, B.; Petersson, G. A.; Nakatsuji, H.; Caricato, M.; Li, X.; Hratchian, H. P.; Izmaylov, A. F.; Bloino, J.; Zheng, G.; Sonnenberg, J. L.; Hada, M.; Ehara, M.; Toyota, K.; Fukuda, R.; Hasegawa, J.; Ishida, M.; Nakajima, T.; Honda, Y.; Kitao, O.; Nakai, H.; Vreven, T.; Montgomery, J. A., Jr.; Peralta, J. E.; Ogliaro, F.; Bearpark, M.; Heyd, J. J.; Brothers, E.; Kudin, K. N.; Staroverov, V. N.; Kobayashi, R.; Normand, J.; Raghavachari, K.; Rendell, A.; Burant, J. C.; Iyengar, S. S.; Tomasi, J.; Cossi, M.; Rega, N.; Millam, N. J.; Klene, M.; Knox, J. E.; Cross, J. B.; Bakken, V.; Adamo, C.; Jaramillo, J.; Gomperts, R.; Stratmann, R. E.; Yazyev, O.; Austin, A. J.; Cammi, R.; Pomelli, C.; Ochterski, J. W.; Martin, R. L.; Morokuma, K.; Zakrzewski, V. G.; Voth, G. A.; Salvador, P.; Dannenberg, J. J.; Dapprich, S.; Daniels, A. D.; Farkas, Ö.; Foresman, J. B.; Ortiz, J. V.; Cioslowski, J.; Fox, D. J. Gaussian 09, revision C.01; Gaussian, Inc.: Wallingford, CT, 2009.
(52) *Gauss View 5.0.9*; GaussView, Gaussian Inc.: Pittsburgh, PA, USA, Copyright 2000-2003 Semichem. Inc.
(53) Gatfaoui, S.; Issaoui, N.; Roisnel, T.; Marouani, H. A proton transfer compound template phenylethylamine: Synthesis, a collective experimental and theoretical investigations. *J. Mol. Struct.* **2019**, *1191*, 183−196.

https://doi.org/10.1021/acsomega.1c02570
ACS Omega 2021, 6, 22603−22615